Terminal cisternae of denervated rabbit skeletal muscle: alterations of functional properties of Ca^{2+} release channels

FRANCESCO ZORZATO, POMPEO VOLPE, ERNESTO DAMIANI, DANIELA QUAGLINO, JR., AND ALFREDO MARGRETH
Centro di Studio per la Biologia e la Fisiopatologia Muscolare del Consiglio Nazionale delle Ricerche, Istituto di Patologia Generale dell'Universita'di Padova, 35131 Padua; and Istituto di Patologia Generale dell'Universita'di Modena, 41100 Modena, Italy

ZORZATO, FRANCESCO, POMPEO VOLPE, ERNESTO DAMIANI, DANIELA QUAGLINO, JR., AND ALFREDO MARGRETH. *Terminal cisternae of denervated rabbit skeletal muscle: alterations of functional properties of Ca^{2+} release channels.* Am. J. Physiol. 257 (Cell Physiol. 26): C504–C511, 1989.—Terminal cisternae (TC) of skeletal muscle represent the specialized compartment from which Ca^{2+} is released into the myoplasm after a propagated action potential. In this study we have investigated the morphology, protein composition, and Ca^{2+} release properties of TC isolated from rabbit gastrocnemius muscle 2 wk after nerve sectioning. Thin-section electron microscopy showed that TC vesicles from denervated muscle were enriched in calsequestrin (CS) and contained a larger fraction of the junctional sarcoplasmic reticulum (SR), as judged by membrane profiles with morphologically intact feet structures. Accordingly, the yield of junctional SR from denervated muscle was twice that of control muscle, and the protein pattern of TC vesicles exhibited an increase in junctional protein components, e.g., CS and the 350-kDa protein. The larger content of the 350-kDa protein, or ryanodine receptor (F. A. Lai, H. Erickson, E. Rousseau, Q.-Y. Liu, and G. Meissner. *Nature Lond.* 331: 315–319, 1988; T. Imagawa, J. S. Smith, R. Coronado, and K, P. Campbell. *J. Biol. Chem.* 262: 10636–10643, 1987; L. Hymel, M. Inui, S. Fleischer, and H. Schindler. *Proc. Natl. Acad. Sci. USA* 85: 441–445, 1988) was paralleled by an increased binding site density (B_{max}) for ryanodine binding in denervated muscle TC. The effects of ruthenium red, a Ca^{2+} release blocker, on Ca^{2+} loading rate and Ca^{2+}-ATPase activity suggested that TC from denervated muscle were less permeable to Ca^{2+}. After active Ca^{2+} loading, both doxorubicin and caffeine induced Ca^{2+} release from isolated TC, yet Ca^{2+} release rates were reduced in denervated muscle TC. This study provides evidence that denervation causes *1*) proliferation of the junctional SR and *2*) significant modifications of the functional properties of the Ca^{2+} release channels of isolated TC.

sarcoplasmic reticulum; denervation; excitation-contraction coupling

IN A PREVIOUS STUDY, we have shown that denervation of rabbit gastrocnemius induces proliferation of transverse tubules (TT), a selective overdevelopment of the cisternal portion of the sarcoplasmic reticulum (SR), and an increase in the number of triads (31). Morphologically, changes of SR membranes in situ are paralleled by marked modifications in protein composition and properties of isolated "heavy" SR fractions (31), indicating that the early effects of denervation on SR membranes concern mainly the junctional region of terminal cisternae (TC). Recently, Saito et al. (30) have described a procedure for the isolation of a SR fraction highly enriched in TC vesicles, containing two types of membranes, the extrajunctional Ca^{2+} pump membrane (~80%) and the junctional face membrane (JFM) or junctional SR (~20%) with morphologically intact feet structures. Purified TC fractions contain calsequestrin (CS), the intraluminal, high-capacity Ca^{2+} binding protein, and are enriched in Ca^{2+} release channels (2). Such Ca^{2+} release channels seem to be restricted to the junctional SR, as indicated by single channel recording of the purified ryanodine receptor[1] incorporated in the lipid bilayer (13, 14, 17).

Previous biochemical studies on the isolated SR from denervated muscle of the rat (26) and of the chicken (36) had concerned mainly the Ca^{2+}-ATPase, but very little is known concerning the Ca^{2+} release properties of TC in denervated muscle. We addressed this issue by studying the protein composition, morphology, and Ca^{2+} release properties of isolated TC from rabbit gastrocnemius 2 wk after denervation. We provide additional and direct evidence that denervation induces an increase of the junctional SR membrane relative to the Ca^{2+} pump membrane. Our results also indicate that TC of denervated muscle are less permeable to Ca^{2+} and less sensitive to both caffeine and doxorubicin, two Ca^{2+} releasing agents (25, 41).

MATERIALS AND METHODS

Materials. Pyruvate kinase and lactate dehydrogenase were obtained from Boehringer (Manneheim, FRG) and phosphocreatine, creatine phosphate kinase, antipyrylazo III, caffeine, and ruthenium red (RR) were obtained from Sigma Chemical (St. Louis, MO). Doxorubicin was a gift from Farmitalia Carlo Erba (Nerviano, Italy). [^{3}H]ryanodine was purchased from New England Nuclear (Dreieich, FRG). Ryanodine was a gift of Dr. Larry R. Jones (Indiana Univ., Indianapolis, IN).

Denervation. Denervation of the gastrocnemius was

[1] The molecular weight of the feet protein has not been determined yet, and it has been reported to be either 450 kDa (14), ~400 kDa (17), 360 kDa (13), or 325 kDa (15). Throughout the text, we shall refer to the feet protein as the 350-kDa protein (40) or ryanodine receptor (13, 14, 17).

obtained by transecting the common popliteal nerve and removing 0.5 cm of the nerve (31). After 2 wk, the animals were killed by cervical dislocation. The muscle from the unoperated leg was used as control.

Purification of TC and JFM-CC fractions. TC were isolated from denervated and control gastrocnemius and were purified by sucrose density gradient centrifugation as described by Saito et al. (30). JFM with compartmental content (JFM-CC) was obtained by Triton X-100 treatment of the TC fraction, as described by Costello et al. (3) and as detailed by Zorzato et al. (40). TC and JFM-CC fractions were resuspended in 0.3 M sucrose and 5 mM imidazole, pH 7.4, and stored at −70°C until used. Protein concentration was determined according to Lowry et al. (19), using bovine serum albumin as standard.

Electron microscopy. TC fractions were prefixed at room temperature with 0.5% glutaraldehyde in Tyrode's buffer plus 0.5% tannic acid and centrifuged. Pellets were fixed with 2.5% glutaraldehyde in Tyrode's for 1 h, treated with OsO_4 in Tyrode's buffer for 30 min at room temperature, dehydrated in ethanol, and embedded in durcupan. Sections were stained with 3% uranyl acetate in 50% ethanol and lead citrate. Observations were made with a Philips 400T electron microscope.

Sodium dodecyl sulfate-polyacrylamide slab gel electrophoresis (SDS-PAGE). SDS-PAGE was carried out according to Laemmli (16) in 5–15% polyacrylamide linear gradient gels. Slab gels were stained with Coomassie brilliant blue. Densitometric scanning of slab gels was carried out in a Gilford spectrophotometer as described previously (31).

CS content of TC fractions was determined as previously described (37), with reference to calibration curves obtained with 0.5–10 μg of purified CS. After SDS-PAGE and Stains All staining (32), the absorbance of each CS band was measured at 615 nm.

Ca^{2+} loading and Ca^{2+}-ATPase activities. Ca^{2+} loading was measured in a Hewlett-Packard 8451A spectrophotometer following the change in absorbance (ΔA) (710–790 nm) of the metallochromic indicator antipyrylazo III. The assays were carried out at either 25 or 30°C in a medium containing, in a final volume of 1 ml, 92 mM K phosphate, pH 7.0, 200 μM antipyrylazo III, either 1 or 2 mM MgATP, 0.5 mM phosphoenolpyruvate, 2.5 units of pyruvate kinase, 2.5 units of lactate dehydrogenase, and 30 μg of TC protein. The reaction was started by adding 50 μM $CaCl_2$.

Adenosinetriphosphatase (ATPase) activity was measured spectrophotometrically by an enzyme-coupled assay following the oxidation of NADH, under the same experimental conditions used for the Ca^{2+} loading assay. Mg^{2+}-ATPase activity was measured in the presence of 0.2 mM ethylene glycol-bis(β-aminoethyl ether)-*N,N,N′,N′*-tetraacetic acid (EGTA). Ca^{2+}-ATPase activity was determined as the difference between total ATPase (0.2 mM $CaCl_2$) and Mg^{2+}-ATPase activities (41).

Ca^{2+} release from TC. Ca^{2+} release measurements were carried out as described by Palade (25). TC fractions were preloaded with ~2 μmol Ca^{2+}/mg protein at 37°C in a medium containing, in a final volume of 1 ml, 7.5 mM sodium pyrophosphate, 2 mM MgATP, 200 μM antipyrylazo III, 100 mM KCl, 5 mM Na_2 creatine phosphate, 20 μg/ml creatine phosphokinase, and 40–50 μg of TC protein. Ca^{2+} loading was performed by adding sequential 25- to 50-nmol $CaCl_2$ pulses. After completion of Ca^{2+} loading, when steady state was attained, Ca^{2+} release was triggered by adding either caffeine (25) or doxorubicin (41).

[^{3}H]ryanodine binding assay. [^{3}H]ryanodine binding assay was performed essentially as described by Fleischer et al. (8) in a medium containing, in a final volume of 1 ml, 0.15 M KCl, 10 mM *N*-2-hydroxyethylpiperazine-*N′*-2-ethanesulfonic acid (HEPES), pH 7.4, and 3 mM ATP as recommended by Campbell et al. (1). [^{3}H]ryanodine was diluted with carrier to obtain a specific radioactivity of 5,000–10,000 dpm/pmol. TC vesicles (0.2 mg/ml) were incubated for 1 h at 37°C with varying concentrations of ryanodine (1 nM–1 μM). Bound [^{3}H]ryanodine was measured by Millipore filtration (0.22-μm Millipore filters). Filters were rinsed with 20 volumes of ice-cold buffer and 10 volumes of 10% ice-cold ethanol (8). Nonspecific binding was determined in the presence of 10 μM cold ryanodine.

RESULTS

Morphology and yield of isolated TC fractions from control and denervated muscle. Morphology and purity of TC fractions were assessed by thin-section electron microscopy. TT, plasma membrane, and mitochondria appeared to be virtually absent from TC isolated both from control and denervated muscle (30; Fig. 1). TC fractions consisted of vesicles having the membrane ultrastructural features and intraluminal electron-dense content, i.e., CS, as previously described (10, 30; Fig. 1). After staining with tannic acid, the Ca^{2+} pump membrane of TC appeared as an asymmetric trilayer, due to the unidirectional alignment of the Ca^{2+}-ATPase molecules, and JFM was characterized by the presence of repeated, but separated, square-shaped units, referred to as junctional feet (30).

The TC fraction from denervated muscle (Fig. 1*B*), when compared with control TC (Fig. 1*A*), appeared enriched of vesicles almost filled with electron-dense material (CS) always attached to the JFM (Fig. 1*C*; see Ref. 10). At higher magnification, the JFM with morphologically intact feet structures was identified in control and denervated TC vesicles (Fig. 1, *A* and *C*, *insets*). The JFM, both the external and internal leaflet in contact with the electron dense material, appeared to be more expanded in TC vesicles from denervated muscle.

The yield of TC (mg protein/50 g muscle) from denervated muscle increased compared with control muscle (Table 1). Interestingly, and in agreement with ultramicroscopic observations (Fig. 1), the yield of JFM-CC from denervated muscle was doubled compared with control muscle (Table 1).

Protein composition and [^{3}H]ryanodine binding of TC fractions from denervated and control muscle. The protein profile of TC membranes further indicated that denervation induces proliferation of the junctional SR relative

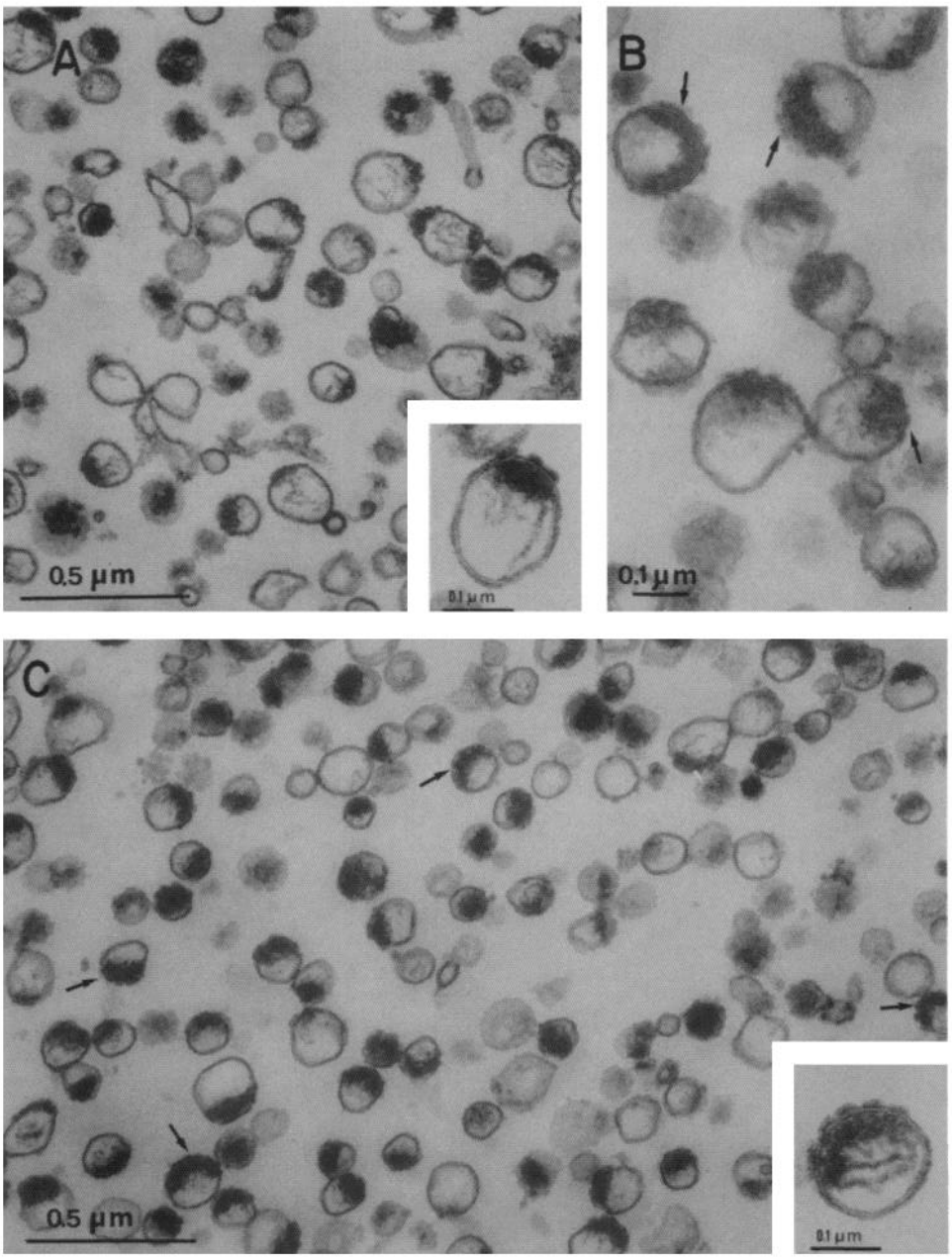

FIG. 1. Thin-section electron microscopy of TC fractions from control (*A*) and denervated muscle (*B* and *C*). Denervation induced an increase of number of CS-containing vesicles and a significant expansion of junctional SR, i.e., membrane area bearing feet projections on external leaflet and electron-dense CS aggregates on inner leaflet (arrows in *B* and *C*). Ultrastructural organization of feet projections is seemingly unaltered in TC from denervated muscle (compare *A* and *C*, *insets*).

TABLE 1. *Yield of TC and JFM-CC fractions from control and denervated muscle*

Fraction	Control Muscle	Denervated Muscle
TC		
mg Protein/50 g muscle	8.0±1 (6)	15.0±2.5* (6)
JFM-CC		
% TC protein	45 (3)	53 (3)
mg Protein/50 g muscle	3.60 (3)	7.95 (3)

Values are means ± SE when >4 preparations were tested, with no. of different SR preparations examined in parentheses. Contralateral muscles were used as control. * $P < 0.01$.

to the Ca^{2+} pump membrane. TC from denervated muscle showed a significant increase of CS and a decrease of the Ca^{2+}-ATPase, as indicated by SDS-PAGE (Fig. 2*B*). Determinations of the CS content by Stains All staining of SDS-PAGE (see MATERIALS AND METHODS for details), indicated that TC of denervated muscle contain more CS than TC of control muscle (46.5 and 31.7%, respectively; see also Ref. 31). Moreover, both the ratio of the 350-kDa protein to the Ca^{2+}-ATPase and the CS/Ca^{2+}-ATPase ratio were increased in TC from denervated muscle (Table 2). Thus the content of two junctional proteins, CS and the 350-kDa protein or ryanodine receptor[1] (13, 14, 17), is increased in TC from denervated muscle.

Direct binding studies with [^{3}H]ryanodine (Fig. 3) likewise demonstrated an increased density of receptor sites in isolated TC from denervated muscle. Scatchard plot analysis of the paired data from denervated and control muscle of three different rabbits indicated a two- to threefold increase in binding site density (B_{max}) (from 5.8 to 14.9 pmol/mg protein, on average). On the other

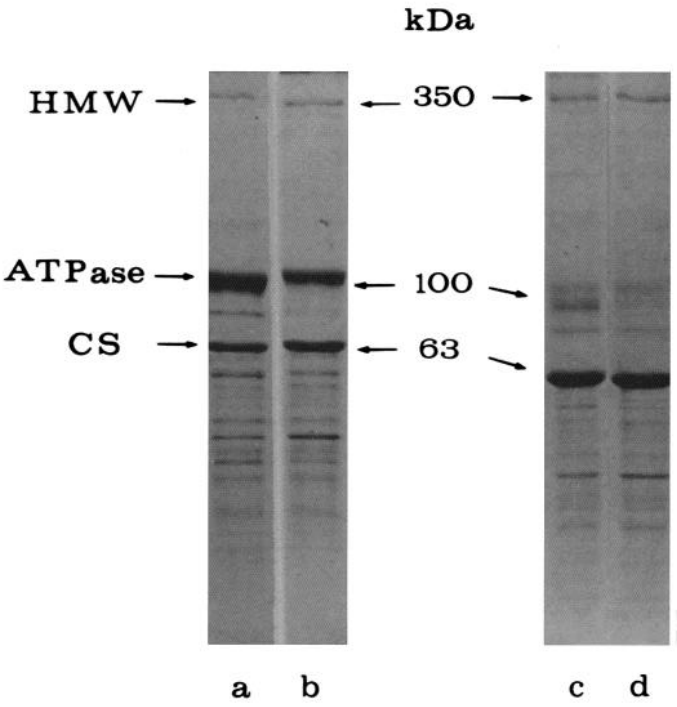

FIG. 2. SDS-PAGE of TC and JFM-CC fractions from control and denervated muscle. 15 μg of protein of each fraction were separated using a linear polyacrylamide gel gradient (5–15%), according to Laemmli (16). Apparent molecular masses are indicated by arrows. TC (*lane a*) and JFM-CC (*lane c*) from control muscle; TC (*lane b*) and JFM-CC (*lane d*) were from denervated muscle. 350-kDa protien/CS ratio, as determined by densitometry (see Table 2), was similar in both TC and JFM-CC from either control or denervated muscle (0.138 and 0.140, respectively). HMW, high-molecular weight protein or 350-kDa protein; ATPase, Ca^{2+}-ATPase.

TABLE 2. *Content of 350-kDa protein, Ca^{2+}-ATPase, and CS of TC fractions from control and denervated muscle*

	350-kDa/Ca^{2+}-ATPase Ratio	CS/Ca^{2+}-ATPase Ratio
Control	0.08±0.02	0.58±0.04
Denervated	0.13±0.01	0.93±0.03

Values are means ± SE; $n = 7$ different preparations. Densitometry of Coomassie blue-stained slab gels was performed as described in MATERIALS AND METHODS. Ratios were calculated by 2 methods: *1*) paper relative to area of each peak was weighted and *2*) area of each peak was determined by triangulation. CS and 350-kDa protein are components of junctional SR. Ca^{2+}-ATPase is a component of free or nonjunctional SR.

hand, there appeared to be retention after denervation of a single, high-affinity [^{3}H]ryanodine binding site. K_d values were also found to be in the same range for control and denervated muscle (see Fig. 3 legend).

When purified junctional SR fractions were analyzed by SDS-PAGE (Fig. 2, *C* and *D*), no appreciable differences in peptide pattern could be detected between control and denervated muscle. The ratio of the 350-kDa protein to CS was found to be closely similar, as determined by densitometry (see Fig. 2 legend).

Ca^{2+} loading by TC from denervated and control muscle. Isolated TC are characterized (2) by low Ca^{2+} rates at low free Mg^{2+} concentrations (~0.1 mM), which can be stimulated five- to sixfold by RR, a Ca^{2+} release blocker.

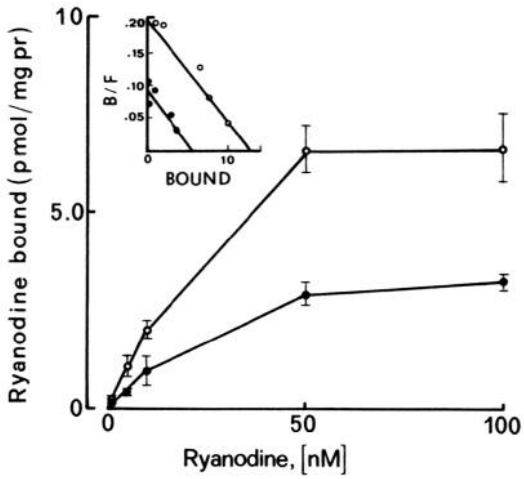

FIG. 3. Binding of ryanodine to TC fractions from control (●) and denervated (○) muscle. Ryanodine binding was performed essentially as described by Fleischer et al. (8), as detailed in MATERIALS AND METHODS. Each data point represents mean ± SD of duplicate determinations carried out on 3 different TC preparations from denervated and control muscle. Mean values at each ryanodine concentration were used to build Scatchard plot (*inset*). B_{max} and K_d values ± SE ($n = 3$) were 5.8 ± 0.5 and 14.9 ± 2.0 pmol/mg protein and 58.3 ± 14.4 and 65.7 ± 14.4 nM for control and denervated TC, respectively. Differences in B_{max} values were found to be significant for $P < 0.01$.

Figure 4 shows the dose-response curve of RR-stimulated Ca^{2+} loading rate in the presence of either 1 or 2 mM total Mg^{2+}. Denervated and control TC were maximally stimulated at 10 μM RR. In the presence of 1 mM Mg^{2+}, TC from control muscles exhibited a fourfold stimulation that was twice as high as that found for TC from denervated muscle (see Table 3, first column). These differences appeared to be independent of changes in the K_m for RR in denervated TC, since K_m values appeared to be similar (Fig. 4*A*, *inset*), and were also comparable to those reported by Chu et al. (2) under similar assay conditions.

Mg^{2+} is an effective inhibitor of Ca^{2+} release from TC (21). As shown in Fig. 4*B*, at 2 mM total Mg^{2+} the stimulatory effect of RR on Ca^{2+} loading rate was reduced by 50% in both TC fractions, even though the maximal stimulation of Ca^{2+} loading rate by RR appeared to be higher in control TC, compared with TC from denervated muscle.

The degree of stimulation of Ca^{2+} loading rate of TC by RR depends on the open-closed state of Ca^{2+} release channels (2, 39): the effect of RR is maximal when a large proportion of Ca^{2+} channels are kept open. Because the K_m for RR was unchanged, the reduced stimulation displayed by TC from denervated muscle could reflect a decreased Ca^{2+} efflux via Ca^{2+} release channels.

Ca^{2+}/ATP coupling ratio of TC from denervated and control muscle. TC fractions exhibit a considerable Ca^{2+} efflux in the absence of RR, and Ca^{2+} loading rate is low under these conditions despite an appreciable Ca^{2+}-dependent ATPase, i.e., transport and catalytic activities are uncoupled, particularly at low free Mg^{2+} (0.1 mM). Ca^{2+}/ATP coupling ratios approached theoretical values of 2 in the presence of RR (2).

Therefore we compared the permeability to Ca^{2+} of control and denervated TC by determining the Ca^{2+}/

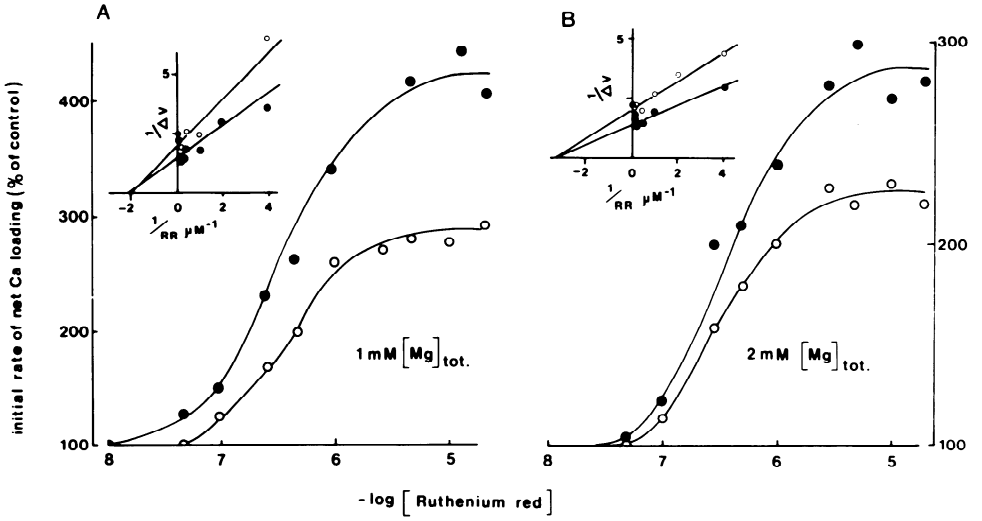

FIG. 4. Effect of RR on Ca^{2+} loading rate of TC fractions from control (●) and denervated (○) muscle. Ca^{2+} loading rates were measured as described in MATERIALS AND METHODS, using antipyrylazo III as Ca^{2+} indicator. Duplicate determinations were carried out on 2 different preparations. Reaction was started by adding 50 μM $CaCl_2$ to a medium containing, in a final volume of 1 ml, 50 μg of TC protein, 100 mM K phosphate, pH 7.0, and either 1 mM MgATP (*A*) or 2 mM MgATP (*B*), at 30°C. Basal rate was subtracted from RR-stimulated rate to give change in rate (ΔV).

ATP coupling ratios at 0.1 mM free Mg^{2+} in the presence and in the absence of 10 μM RR. The maximal Ca^{2+} loading rate of TC was 30% lower for denervated compared with control muscle (Table 3). However, because the Ca^{2+}-dependent ATPase activity of denervated TC decreased to a similar extent, the Ca^{2+} transport efficiency appeared to be unchanged, as indicated by the high Ca^{2+}/ATP coupling ratio (Table 3).

In the absence of RR, Ca^{2+} loading rates of both TC fractions were similar, but the Ca^{2+}/ATP coupling ratio of denervated TC was ~30% higher, indicating that TC fractions from denervated muscle are less permeable to Ca^{2+}. Analysis of the data of Table 3, according to Feher and Lipford (6), indicates that the percentage of RR-sensitive (Ca^{2+} channel containing) vesicles is similar for TC of control and denervated muscle (58 and 55%, respectively; see Table 3 legend for details). Thus the higher Ca^{2+}/ATP coupling ratio is not due to a change in the percentage of vesicles sensitive to RR.

TABLE 3. *Functional properties of TC fractions from denervated and control muscle*

	Ca^{2+} Loading Rate, μmol Ca^{2+}·min^{-1}·mg^{-1}	Ca^{2+}-ATPase Activity, μmol P_i·min^{-1}·mg^{-1}	Ca^{2+}/ATP Coupling Ratio
Control			
− RR	0.18±0.02 (6)	0.73±0.12 (6)	0.28±0.04 (6)
+ RR	0.88±0.10 (6)	0.63±0.10 (6)	1.45±0.25 (6)
+ Doxorubicin	0.14 (2)	1.20 (2)	0.11 (2)
+ Caffeine	0.15 (2)	1.25 (2)	0.11 (2)
Denervated			
− RR	0.21±0.02* (6)	0.51±0.10 (6)	0.41±0.05† (6)
+ RR	0.64±0.07† (6)	0.46±0.07 (6)	1.50±0.20* (6)
+ Doxorubicin	0.17 (2)	1.05 (2)	0.15 (2)
+ Caffeine	0.17 (2)	0.90 (2)	0.17 (2)

Values are means ± SE when >4 TC preparations were tested, with no. of different SR preparations examined in parentheses. Ca^{2+} loading rate and Ca^{2+}-dependent ATPase activity were measured at 25°C using an identical assay medium as described in MATERIALS AND METHODS. Coupling ratio is ratio between Ca^{2+} loading rate and Ca^{2+}-dependent ATPase activity. Total Mg^{2+} concentration was 1 mM and corresponds to a free Mg^{2+} concentration of ~0.1 mM. RR, doxorubicin, and caffeine were 10 μM, 100 μM, and 20 mM, respectively. Percentage of vesicles containing Ca^{2+} release channels is calculated using Ca^{2+}/ATP coupling ratios measured in presence and absence of RR, as outlined by Feher and Lipford (6). Three classes of vesicles are considered: vesicles sensitive to RR and containing Ca^{2+} release channels (V_c), vesicles insensitive to RR and lacking Ca^{2+} channels (V_i), and leaky vesicles (V_l). If ideal coupling ratio (η) is 2.0 and C_c and C_i are the measured Ca^{2+}/ATP coupling ratios in presence and absence of RR, respectively, then following equation system can be written: $V_c + V_i + V_l = 100$; $C_i = \eta V_i$; and $C_c = \eta(V_i + V_c)$. Therefore for control TC fraction, V_c = 58%, V_i = 14%, and V_l = 28%; for denervated TC fraction, V_c = 55%, V_i = 20%, and V_l = 25%. * NS; † $P < 0.05$.

Doxorubicin and caffeine are Ca^{2+}-releasing agents that most likely act by opening Ca^{2+} release channels of TC (25, 41), thus decreasing net Ca^{2+} loading rate. In the presence of either 100 μM doxorubicin or 20 mM caffeine, the Ca^{2+}/ATP coupling ratios were low as expected, yet the values for denervated TC were still higher than those for control TC (Table 3). These results indirectly suggest that TC from denervated muscle are less sensitive to Ca^{2+} releasing agents.

Ca^{2+} release from TC of denervated and control muscle. In search of an explanation for the observed differences in Ca^{2+} permeability properties, we studied drug-induced Ca^{2+} release from TC fractions.

In preliminary experiments it was found that Ca^{2+} release rates were related to the amount of Ca^{2+} preloading and that maximal release rates were attained above 1.8 μmol/mg protein for both control and denervated TC (data not shown). In the experiments of Figs. 5 and 6, TC from either control or denervated muscle were actively loaded with ~2 μmol Ca^{2+}/mg protein and when steady state was attained, Ca^{2+} releasing agents were added (25). Figure 5 shows two typical tracings for control (*A*) and denervated TC (*B*): after active Ca^{2+} preloading, 50 μM doxorubicin evoked Ca^{2+} release from both control and denervated TC, yet Ca^{2+} release rate was higher for control TC (*A*). Figure 6 shows the effect of caffeine (*A*) and doxorubicin (*B*) on the initial rate of Ca^{2+} release from control and denervated TC. Half-maximal stimulation of caffeine-induced Ca^{2+} release was attained at 8 and 10 mM for denervated and control TC, respectively. At saturating concentrations of either caffeine or doxorubicin, the initial rates of Ca^{2+} release from control TC were twofold higher than those of denervated TC. In additional experiments carried out at

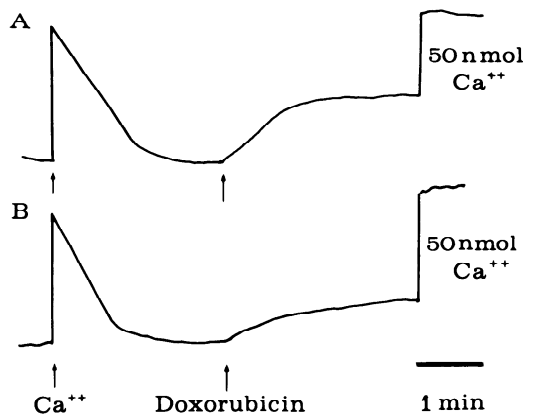

FIG. 5. Doxorubicin-induced Ca^{2+} release from TC fractions of control and denervated muscle. Ca^{2+} loading and Ca^{2+} release were measured as described in MATERIALS AND METHODS, using antipyrylazo III as Ca^{2+} indicator. Assay was started by adding ~50 μg of protein of control TC (*A*) and denervated TC (*B*). Two consecutive 50-nmol $CaCl_2$ pulses were administered, and 2nd pulse is shown (Ca^{2+}). After completion of Ca^{2+} loading, 50 μM doxorubicin was added. A downward deflection of absorbance tracings is indicative of Ca^{2+} loading; an upward deflection corresponds to Ca^{2+} release. At end of each experiment, one 50-nmol $CaCl_2$ pulse was added to recalibrate dye response.

lower Ca^{2+} preloading level (0.5 and 1 μmol Ca^{2+}/mg protein), the observed differences between control and denervated TC were even larger (data not shown).

DISCUSSION

A long-described, early membrane response to the loss of motor innervation to the muscle, seen in amphibian (24) and mammalian (5, 27, 34) twitch fibers and shared also by invertebrate insect muscle (29), is the increase in volume and surface development of TC, as longitudinal network of SR becomes simplified. As reinvestigated recently in isolated muscle fractions from the gastrocnemius of the rabbit (31), changes within the SR membrane system between 1 and 3 wk after denervation appear to occur concomitantly with the proliferation of transverse tubules (27).

Our present results demonstrate time correlated changes in membrane composition and in the Ca^{2+} release properties of isolated TC, 2 wk after denervation.

Proliferation of junctional SR after denervation. An overdevelopment of the junctional SR, relative to the Ca^{2+} pump membrane, after muscle denervation is supported by the following lines of evidence: *1*) TC from denervated muscle are enriched in vesicles with morphologically intact feet structures and contain larger masses of electron-dense compartmental contents, i.e., CS (Fig. 1); *2*) differences in protein profile between the TC fractions of denervated and contralateral control muscle are mainly referable to a twofold increase in the ratio of CS to Ca^{2+}-ATPase protein and to a corresponding increase in the relative amount of the 350-kDa feet protein, a specific marker of the junctional SR, recently identified as the ryanodine receptor (13, 14, 17); and *3*) [^{3}H]ryanodine binding studies demonstrate a parallel increase of ryanodine binding sites in isolated TC from denervated muscle, as deduced from changes in B_{max} values.

Single-channel recording studies have shown that the ryanodine receptor is a Ca^{2+} release channel (13, 14, 17)

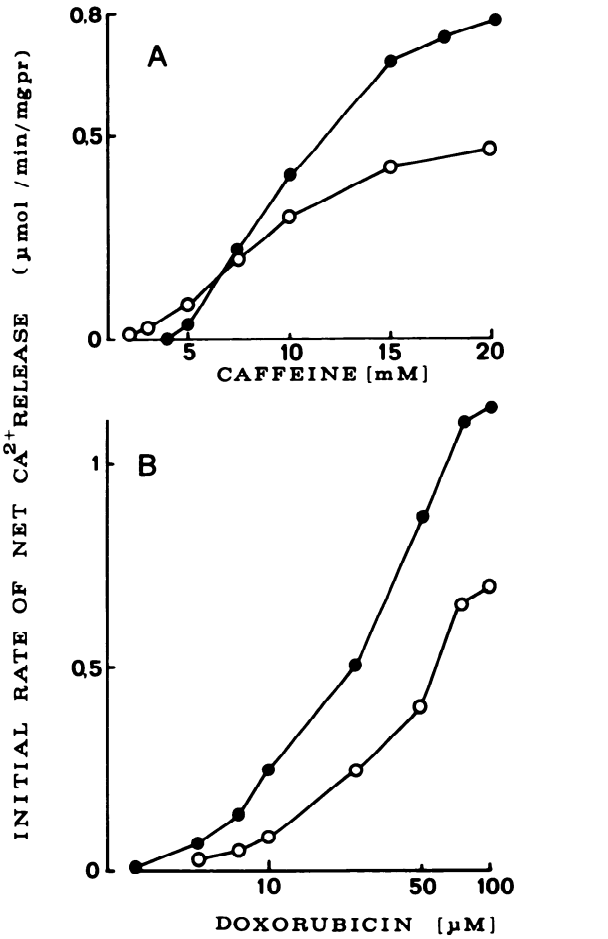

FIG. 6. Drug-induced Ca^{2+} release from isolated TC fractions of control and denervated muscle. Both TC fractions (40 μg protein) were preloaded with 2 μmol Ca^{2+}/mg protein in a medium containing, in a final volume of 1 ml, 7.5 mM pyrophosphate, pH 7.0, 2 mM MgATP, 200 μM antipyrylazo, 100 mM KCl, 5 mM disodium creatine phosphate, and 20 μg/ml creatine kinase. Increasing concentrations of caffeine (*A*) and of doxorubicin (*B*) were added after completion of Ca^{2+} accumulation. At end of each experiment, one 50-nmol $CaCl_2$ pulse was added to recalibrate dye response. Duplicate determinations were carried out on TC from control muscle (●) and denervated muscle (○).

that seems to exist as a tetrametric complex of 350-kDa subunits (17). Because TC from denervated muscle have a higher B_{max} for ryanodine, it appears that denervation induces an increase in the number of Ca^{2+} release channels. TC from denervated muscle bind ryanodine with the same affinity as control TC. However, this finding per se does not warrant the conclusion that the Ca^{2+} channel subunit composition is identical in control and denervated muscle.

Reduced Ca^{2+} permeability of TC after denervation. The occurrence of changes in the functional properties of the Ca^{2+} release channels of junctional SR after denervation of the muscle is strongly implied by the data reported in Figs. 4–6 and Table 3. *1*) TC from denervated muscle are functionally distinct in that they have a relatively high ATP-dependent Ca^{2+} loading when normalized for the content of Ca^{2+}-ATPase protein, which is enhanced to a lower extent, i.e., about one-half as much compared with control, by RR, which locks the Ca^{2+} channels in a closed configuration (2, 39), as well as by high Mg^{2+}, likewise known to be an effective inhibitor of Ca^{2+} release from

TC (21). 2) The rate of both caffeine- and doxorubicin-induced Ca^{2+} release is reduced after denervation. Because the affinity for either doxorubicin, caffeine, or RR is not changed, it appears that after denervation Ca^{2+} release channels are predominantly in an inactivated and/or closed configurational state (23).

The relevance of our present findings to the altered Ca^{2+} homeostasis and prolongation of isometric twitch of skeletal muscle early after denervation (28), before changes in the intrinsic properties of the contractile proteins (4, 7), must be assessed in the framework of previous experimental findings. Changes in the time course of the contraction-relaxation cycle in fast-twitch fibers deprived of their motor innervation are likely to involve changes both in the amount and in the rate of Ca^{2+} release and in the rate of ATP-dependent Ca^{2+} uptake as well as possibly in the excitation-coupling process itself (4).

The finding of an increased Ca^{2+} content in denervated muscle (28), on account of our present and previous evidence (31), is best explained by an increase in size of the Ca^{2+} pool within the TC compartment of the SR, the Ca^{2+} being probably present in CS-bound form, since intraluminal CS is found considerably augmented. Contrastingly, the Ca^{2+} binding protein parvalbumin decreases in the myoplasm of denervated muscle (18). An increase in the amount of stored Ca^{2+} within the lumen of the SR, together with an increase in number of Ca^{2+} release sites per muscle fiber and per sarcomere (31), would be expected per se to shorten the duration of the muscle active state, unless the rate of Ca^{2+} release is markedly reduced. Although ATP-dependent Ca^{2+} transport across SR membranes appears to be tightly coupled and there is likewise no evidence of a fast to slow change of the SR Ca^{2+}-ATPase in rabbit gastrocnemius after denervation (31), there is, however, evidence that total number of Ca^{2+} pump units per fiber decreases, which would imply a concomitant decrease in the rate of Ca^{2+} reuptake from the myoplasm.

Caffeine-induced contracture is a property shared by mammalian slow-twitch and denervated fast-twitch fibers (12). Differences in the dose-response effect of doxorubicin on the rate of tension rise between chemically skinned slow and fast muscle fibers have been observed (32), which superficially bear some resemblance to those reported here for doxorubicin-induced Ca^{2+} release between isolated TC from denervated and control gastrocnemius. However, twitch potentiation elicited by low concentrations of caffeine was reported to be similar for denervated and normal fast muscle (12), and drug-responses of skinned fast and slow fibers differ in many other significant ways (32). Thus it seems unjustified, at the present time, to explain the reduced Ca^{2+} permeability of TC after muscle denervation as being truly equivalent to a fast to slow transition.

Does motor innervation control Ca^{2+} release isochannel transitions? Well-described, early changes in properties and composition of the surface membrane of muscle fibers after denervation are the development of tetrodotoxin-resistant action potentials (35), as the result of Na^+ channel transitions (11), and the spreading of acetylcholine sensitivity, concomitant with the substitution of the adult, junctional type of acetylcholine receptor channel by the fetal, extrajunctional type (22). An interesting possibility, although entirely speculative at the present time, is that there may exist different subtypes of Ca^{2+} release channels in skeletal muscle SR, according to the type of motor innervation as well as the stage of development of the muscle, and that there may occur isochannel transitions, as a specific effect of the loss of innervation, to account for changes in Ca^{2+} permeability of junctional SR. Although little is known on differences in Ca^{2+} homeostasis between immature fast and denervated adult muscle, it is significant that the development of TT and of junctional SR precedes that of longitudinal SR during postnatal development of fast muscles (20, 33, 38), i.e., before muscle fibers have acquired the twitch characteristics of the adult fast type.

The technical assistance of G. A. Tobaldin is gratefully acknowledged. Thanks are also due to Dr. Charlotte A. Tate (Baylor College of Medicine, Houston, TX) for comments on the manuscript and to Lynette Morgan for typing the manuscript.

This work was supported by institutional funds from the Consiglio Nazionale delle Ricerche and by a grant from Ministero della Pubblica Instruzione to A. Margreth.

Present address of P. Volpe: Department of Physiology and Biophysics, University of Texas Medical Branch, Galveston, TX 77550.

Address for reprint requests: A. Margreth, Istituto di Patologia Generale, via Loredan 16, 35131 Padova, Italy.

Received 19 October 1988; accepted in final form 14 April 1989.

REFERENCES

1. CAMPBELL, K. P., C. M. KNUDSON, T. IMAGAWA, A. T. LEUNG, J. L. SUTKO, S. D. KAHL, C. R. RAAB, AND L. MADSON. Identification and characterization of the high affinity [^{3}H]-ryanodine receptor of the junctional sarcoplasmic reticulum Ca^{2+} release channel. *J. Biol. Chem.* 262: 6460–6463, 1987.
2. CHU, A., P. VOLPE, B. COSTELLO, AND S. FLEISCHER. Functional characterization of junctional terminal cisternae from mammalian fast skeletal muscle sarcoplasmic reticulum. *Biochemistry* 25: 8315–8325, 1986.
3. COSTELLO, B., C. CHADWICK, A. SAITO, A. CHU, A. MAURER, AND S. FLEISCHER. Characterization of the junctional face membrane from terminal cisternae of sarcoplasmic reticulum. *J. Cell Biol.* 103: 741–753, 1986.
4. DULHUNTY, A. F. Excitation-contraction coupling and contractile properties in denervated rat EDL and soleus muscle. *J. Muscle Res. Cell Motil.* 6: 207–225, 1985.
5. ENGEL, A. G., AND H. H. STONNINGTON. Morphological effects of denervation of muscle. A quantitative ultrastructural study. *Ann. NY Acad. Sci.* 228: 68–88, 1974.
6. FEHER, J. J., AND G. B. LIPFORD. Mechanism of action of ryanodine on cardiac sarcoplasmic reticulum. *Biochim. Biophys. Acta* 813: 77–86, 1985.
7. FINOL, H. J., D. M. LEWIS, AND R. OWENS. The effects of denervation on contractile properties of rat skeletal muscle. *J. Physiol. Lond.* 319: 81–92, 1981.
8. FLEISCHER, S., E. OGUNBUNMI, M. C. DIXON, AND E. A. M. FLEER. Localization of Ca^{2+} release channel with ryanodine in junctional terminal cisternae of sarcoplasmic reticulum of fast skeletal muscle. *Proc. Natl. Acad. Sci. USA* 82: 7256–7259, 1985.
9. FOSSET, M. E., E. JAIMOVICH, E. DELPONT, AND M. LAZDUNSKI. [^{3}H]-nitrendipine receptor in skeletal muscle. Properties and preferential localization in transverse tubules. *J. Biol. Chem.* 258: 5086–6092, 1983.
10. FRANZINI-ARMSTRONG, C., L. J. KENNEY, AND E. VARRIANO-MARSTON. The structure of calsequestrin in triads of vertebrate skeletal muscle: a deep etch study. *J. Cell Biol.* 105: 49–56, 1987.
11. GUO, X., A. VEHARA, A. RAVIDRAN, S. H. BRYANT, S. HALL, AND

E. MOCZYDLOWSKI. Kinetic basis for insensitivity to tetrodotoxin and saxitoxin in sodium channels of canine heart and denervated rat skeletal muscle. *Biochemistry* 26: 7546–7556, 1987.

12. GUTMANN, E., AND A. SANDOW. Caffeine-induced contracture and potentiation of contraction in normal and denervated rat muscle. *Life Sci.* 4: 1149–1157, 1965.
13. HYMEL, L., M. INUI, S. FLEISCHER, AND H. SCHINDLER. Purified ryanodine receptor of skeletal muscle sarcoplasmic reticulum forms Ca^{2+}-activated oligomeric Ca^{2+} channels in planar bilayers. *Proc. Natl. Acad. Sci. USA* 85: 441–445, 1988.
14. IMAGAWA, T., J. S. SMITH, R. CORONADO, AND K. P. CAMPBELL. Purified ryanodine receptor from skeletal muscle sarcoplasmic reticulum is the Ca^{2+}-permeable pore of the calcium release channel. *J. Biol. Chem.* 262: 10636–10643, 1987.
15. KAWAMOTO, R. M., J. P. BRUNSCHWIG, K. C. KIM, AND A. H. CASWELL. Isolation, characterization, and localization of the spanning protein from skeletal muscle triads. *J. Cell Biol.* 103: 1405–1414, 1986.
16. LAEMMLI, U. K. Cleavage of structural proteins during the assembly of the head of bacteriophage T4. *Nature Lond.* 227: 680–686, 1970.
17. LAI, F. A., H. ERICKSON, E. ROUSSEAU, Q.-Y. LIU, AND G. MEISSNER. Purification and reconstitution of the calcium release channel from skeletal muscle. *Nature Lond.* 331: 315–319, 1988.
18. LEBERER, E., AND D. PETTE. Neural regulation of parvalbumin expression in mammalian skeletal muscle. *Biochem. J.* 235: 67–73, 1986.
19. LOWRY, O. H., N. J. ROSEBROUGH, A. L. FARR, AND R. J. RANDALL. Protein measurement with the Folin phenol reagent. *J. Biol. Chem.* 193: 265–275, 1951.
20. MARGRETH, A., G. SALVIATI, I. MUSSINI, AND U. CARRARO. Ultrastructure and macromolecular composition of the sarcoplasmic reticulum in relation to the twitch characteristics of skeletal muscle: In: *Exploratory Concepts in Muscular Dystrophy*, edited by A. T. Milhorat. Amsterdam: Excerpta Med., 1974, vol. II, p. 406–418.
21. MEISSNER, G., E. DARLING, AND J. EVELETH. Kinetics of rapid Ca^{2+} release by sarcoplasmic reticulum. Effects of Ca^{2+}, Mg^{2+} and adenine nucleotide. *Biochemistry* 25: 236–244, 1986.
22. MISHINA, M., T. TAKAI, K. IMOTO, M. NODA, T. TAKAHASHI, S. NUMA, C. METHFESSEL, AND B. SAKMANN. Molecular distribution between fetal and adult forms of muscle acetylcholine receptor. *Nature Lond.* 321: 406–411, 1986.
23. MORII, H., H. TAKISAWA, AND T. YAMAMOTO. Inactivation of a Ca^{2+}-induced Ca^{2+} release channel from skeletal muscle sarcoplasmic reticulum during active transport. *J. Biol. Chem.* 260: 11536–11541, 1985.
24. MUSCATELLO, U., A. MARGRETH, AND M. ALOISI. On the differential response of sarcoplasm and myoplasm to denervation in frog muscle. *J. Cell Biol.* 27: 1–24, 1965.
25. PALADE, P. Drug-induced calcium release from isolated sarcoplasmic reticulum. *J. Biol. Chem.* 262: 6135–6141, 1987.
26. PALEXAS, G. N., N. SAVAGE, AND H. ISSACS. Characteristics of sarcoplasmic reticulum from normal and denervated rat skeletal muscle. *Biochem. J.* 200: 11–15, 1981.
27. PELLEGRINO, C., AND C. FRANZINI. An electron microscope study of denervation atrophy in red and white skeletal muscle fibres. *J. Cell Biol.* 17: 327–349, 1963.
28. PICKEN, J. R., AND A. C. KIRBY. Denervated frog skeletal muscle. Calcium content and kinetics of exchanges. *Exp. Neurol.* 53: 64–70, 1976.
29. REES, D., AND P. N. R. USHERWOOD. Effects of denervation on the ultrastructure of insect muscle. *J. Cell Sci.* 10: 667–682, 1972.
30. SAITO, A., S. SEILER, A. CHU, AND S. FLEISCHER. Preparation and morphology of sarcoplasmic reticulum terminal cisternae from rabbit skeletal muscle. *J. Cell Biol.* 99: 875–885, 1984.
31. SALVATORI, S., E. DAMIANI, F. ZORZATO, P. VOLPE, S. PIEROBON, D. QUAGLINO, JR., G. SALVIATI, AND A. MARGRETH. Denervation-induced proliferative changes of triads in rabbit skeletal muscle. *Muscle Nerve* 11: 1246–1259, 1988.
32. SALVIATI, G., AND VOLPE, P. Ca^{2+} release from sarcoplasmic reticulum of skinned fast- and slow-twitch muscle fibers. *Am. J. Physiol.* 254 (*Cell Physiol.* 23): C456–C465, 1988.
33. SCHIAFFINO, S., AND A. MARGRETH. Coordinate development of the sarcoplasmic reticulum and T-system during postnatal differentiation of rat skeletal muscle. *J. Cell Biol.* 41: 855–870, 1969.
34. SCHIAFFINO, S., AND P. SETTEMBRINI. Studies on the effects of denervation in developing muscle. I. Differentiation of sarcotubular system. *Virchows Arch. B Cell Pathol.* 4: 345–356, 1970.
35. SCHMID, A., J. F. RENAUD, M. FOSSET, J. P. MEAUX, AND M. LAZDUNSKI. The nitrendipine-sensitive Ca^{2+} channel in chick muscle cells and its appearance during myogenesis in vitro and in vivo. *J. Biol. Chem.* 259: 11366–11372, 1984.
36. TATE, C. A., R. J. BICK, T. D. MYERS, B. J. PITTS, W. B. VAN WINKLE, AND M. E. ENTMANN. Alteration of sarcoplasmic reticulum after denervation of chicken pectoralis muscle. *Biochem. J.* 210: 339–344, 1983.
37. VOLPE, P., M. BRAVIN, F. ZORZATO, AND A. MARGRETH. Isolation of terminal cisternae of frog skeletal muscle. Calcium storage and release properties. *J. Biol. Chem.* 263: 9901–9907, 1988.
38. VOLPE, P., E. DAMIANI, G. SALVIATI, AND A. MARGRETH. Transition in membrane composition during postnatal development of rabbit fast muscle. *J. Muscle Res. Cell Motil.* 3: 213–230, 1982.
39. VOLPE, P., G. SALVIATI, AND A. CHU. Ca^{2+}-gated Ca^{2+} channels of chemically skinned fibers of the rabbit. *J. Gen. Physiol.* 87: 289–301, 1986.
40. ZORZATO, F., A. MARGRETH, AND P. VOLPE. Direct photoaffinity labeling of junctional sarcoplasmic reticulum with [^{14}C]-doxorubicin. *J. Biol. Chem.* 261: 13252–13257, 1986.
41. ZORZATO, F., G. SALVIATI, T. FACCHINETTI, AND P. VOLPE. Doxorubicin induces calcium release from terminal cisternae of skeletal muscle. *J. Biol. Chem.* 260: 7349–7355, 1985.